Pamukkale Üniversitesi Mühendislik Bilimleri Dergisi
Pamukkale University Journal of Engineering Sciences

Measurement of important tribocorrosion properties of titanium implant and assessment with digital image processing

Titanyum implantının önemli tribokorozyon parametrelerinin ölçümü ve sayısal görüntü işleme ile değerlendirilmesi

Emrah IRMAK[1], Enis KÖRPE[1]*

[1]Department of Electrical and Electronics Engineering, Alanya Alaaddin Keykubat University, Alanya, Türkiye.
emrah.irmak@alanya.edu.tr

Received/Geliş Tarihi: 12.11.2024 Revision/Düzeltme Tarihi: 26.01.2025 doi: 10.5505/pajes.2025.55562
Accepted/Kabul Tarihi: 05.02.2025 Research Article/Araştırma Makalesi

Abstract

Titanium implants are mechanical systems where tribocorrosion is frequently observed at the interface between the implant and the abutment alloy. In this paper, important parameters in terms of tribocorrosion such as abrasion coefficient, abrasion volume loss and corrosion rate were determined experimentally in a laboratory environment by preparing a sufficient number of samples obtained from the field for this material (Titanium-Ti6Al4V), which is actively used in surgeries. Comprehensive analysis of these mechanical systems in body-like environments contributes to a better understanding of the material loss caused by abrasion and corrosion interactions occurring at the interface between the implant and the abutment alloy. The samples were subjected to dry sliding wear with the pin-on-disc system in accordance with the relevant standards for a certain number of cycles, during which abrasion volume loss and friction coefficient were measured simultaneously. The results of these experiments were examined to evaluate the degree to which titanium is resistant to material loss due to abrasion and corrosion in body implants. It was found that the abrasion coefficient decreased by 51% when 10 N load was applied by 22% when 20 N load was applied, and by 2% when 30 N load was applied. The samples screws were exposed to 15% more corrosive abrasion and it was found that they had 6% higher corrosion rate in electrochemical corrosion test. Additionally, the morphological features of the abraided and corroded surfaces of Ti6Al4V alloy were analyzed and interpreted using scanning electron microscopy (SEM) and digital image processing techniques.

Keywords: Titanium, Abrasion, Corrosion, Tribocorrosion, Digital Image Processing, Artificial Body Fluid.

Öz

Titanyum implantlar, implant ile abutment alaşımı arasındaki arayüzde tribokorozyonun sıklıkla görüldüğü mekanik sistemlerdir. Bu çalışmada, cerrahide aktif olarak kullanılan bu malzeme (Titanyum-Ti6Al4V) için sahadan elde edilen yeterli sayıda numune hazırlanarak, aşınma katsayısı, aşınma hacim kaybı ve korozyon hızı gibi tribokorozyon açısından önemli parametreler laboratuvar ortamında deneysel olarak belirlenmiştir. Bu mekanik sistemlerin vücut benzeri ortamlarda kapsamlı analizi, implant ile abutment alaşımı arasındaki arayüzde oluşan aşınma ve korozyon etkileşimlerinin neden olduğu malzeme kaybının daha iyi anlaşılmasına katkıda bulunmaktadır. Numuneler, ilgili standartlara uygun olarak belirli sayıda çevrim boyunca pim-disk sistemi ile kuru kayma aşınmasına tabi tutulmuş ve bu esnada aşınma hacim kaybı ve sürtünme katsayısı eş zamanlı olarak ölçülmüştür. Bu deneylerin sonuçları, titanyumun vücut implantlarında aşınma ve korozyona bağlı malzeme kaybına karşı ne kadar dirençli olduğunu değerlendirmek için incelenmiştir. Aşınma katsayısının 10 N yük uygulandığında %51, 20 N yük uygulandığında %22 ve 30 N yük uygulandığında %2 azaldığı tespit edilmiştir. Numune vidalar %15 daha fazla korozif aşınmaya maruz kalmış ve elektrokimyasal korozyon testinde %6 daha yüksek korozyon oranına sahip oldukları tespit edilmiştir. Ek olarak, Ti6Al4V alaşımının aşınmış ve korozyona uğramış yüzeylerinin morfolojik özellikleri, taramalı elektron mikroskobu (SEM) ve dijital görüntü işleme teknikleri kullanılarak analiz edilmiş ve yorumlanmıştır.

Anahtar kelimeler: Titanyum, Aşınma, Korozyon, Tribokorozyon, Dijital Görüntü İşleme, Yapay Vücut Sıvısı

1 Introduction

Titanium implants are frequently preferred for biomedical applications due to their high durability, corrosion resistance, low density and superior biocompatibility properties. Titanium alloy has the highest chemical affinity to oxygen and carbon elements. Therefore, due to its affinity to carbon element in the first place, Titanium becomes brittle quickly and can form new chemical products at high temperatures and in an oxygen-rich environment [1]. Titanium alloy tends to abrade when it encounters friction between other elements. Corrosion is an undesirable chemical event that forms hydroxide, oxygen and different compounds by reacting with the environment of the Titanium implant. The human body contains ions such as oxygen, protein, fluid water and hydroxide [2]. Therefore, the human body is a corrosive environment for Titanium alloy. Titanium alloy is weakened by corrosion and can damage tissues due to corrosion [3]. Titanium alloys have limited use in engineering applications due to their high coefficient of friction and weakness against abrasion. To improve these poor tribological properties of Titanium alloy, it is necessary to improve the surface properties of Titanium [4].

Tribocorrosion is the study of abrasion and corrosion processes that occur simultaneously on surfaces in contact with each other because of chemical, mechanical (abrasion) and electrochemical (corrosion) interactions [5]. These interactions can lead to both positive and negative results depending on the specific properties of the surfaces and the changes in material properties due to reactions in the simulated environments used.

Titanium alloys cannot be used for a long time due to reasons such abrasion, corrosion and low strength. Therefore, a second

*Corresponding author/Yazışılan Yazar

surgery is needed. These surgeries are expensive and painful for the patient, and the surgeries may not be successful. Therefore, research has been conducted in [7] to develop new alloys to eliminate these problems. In [8], the authors investigated the relationship between heat treatment and TiN coating on the mechanical properties of Titanium alloy. As a result of heat treatment applied to Titanium alloy, the load capacity increased. When only TiN coating was applied, it was observed that the load capacity did not change compared to samples coated with only TiN when both TiN coating and heat treatment were applied. Morphological imaging was performed using SEM and optical microscope. In [9], the effects of thermal oxidation on corrosion and surface properties of CP-Ti and Ti6Al4V alloys were investigated. As a result of thermal oxidation, hardness measurements, optical microscope examinations and X-ray diffraction examinations of untreated original and oxidized samples were performed. The prepared samples were subjected to the Rocwell C indentation test, corrosion test and scratch test. In [10], osteogenic and biocompatible composite nano coatings were developed in the research conducted on Titanium surfaces. Biological, chemical and physical properties of the nano coatings were examined. Hydroxyapatite, poly and strontium ranelate, which are biocompatible and polymer, were used in the coatings. A porous structure was created on the titanium alloy of the developed nanofiber coatings and thus a suitable interface was created for cell viability. In [11], ZrO_2 and HA were prepared at different rates and applied to increase biocompatibility for Titanium and to create bioactive structures on the surface. ZrO_2+HA generally increased the surface roughness. A bioactive Ca/P structure was formed on the surfaces of the samples kept in artificial body fluid. Research was carried out in two different groups to obtain information about the in vitro biocompatibility of Titanium alloy in SVS solutions. The first group was sandblasted with ZrO_2+HA powders, and the second group was surface modified with fat tissue laser. It was seen that the two surface treatments changed the surfaces of the samples and the sandblasting process created a more pronounced rough surface structure compared to the laser process.

Researchers investigated the mechanical properties of Ti6Al4V alloy [12]. The surface roughness of the offset, block and standard size samples produced using the EDE method was examined. The obtained samples were subjected to tensile tests in standard sizes. The mechanical properties of Ti6Al4V alloy before and after production were examined using the EDE method. The high coefficient of friction of the titanium alloy and the low abrasion resistance limit the usage area of the titanium alloy. Therefore, various surface modification processes are applied to improve the abrasion properties of the titanium alloy. In the study [13], the surface properties of pure Titanium (CP-Ti) and Ti6Al4V alloy were developed. While the surface of CP-Ti was coated with Ni-B, nickel and graphene at different rates were coated on the surface of the titanium alloy by pulse current coating method. Surface morphology EDS, SEM, OM and XRD analysis were performed. The obtained Ni-B coating and graphene composite coatings of different sizes showed lower wear rate, higher hardness and higher friction coefficient compared to untreated CP-Ti and Ti6Al4V alloy. In [14], the welding progress speed, which is the heat effect on the welding values of the CO_2 laser welded joint of Ti6Al4V alloy, was investigated. Tensile tests and hardness measurements were performed to investigate the mechanical values by joining the titanium alloy at different welding speeds with the CO_2 laser welding method. In addition, the microstructures of the joints were also examined. In this way, the mechanical properties and microstructures of the joints were examined and the effect of the welding progress speed was investigated. Moreover, the biocorrosion and biocompatibility effects of the Titanium alloy were investigated. Laser-welded Titanium alloys were kept in artificial body fluid and their bioactivity properties were investigated. After the bioactivity test, the hydroxyapatite on the surface was cleaned and weight losses were calculated. Furthermore, biocorrosion rates were found. In the study [15], it was aimed to determine the best temperature and time parameters to improve the surface and mechanical properties of Titanium alloy by carburizing Titanium alloy in Low Pressure Carburizing furnaces at different temperatures and different diffusion times. The best parameters were determined to be the sample carburized at 850 ℃ for 4 hours. The friction coefficient was found to be 0.18. Boronizing of Ti6Al4V alloy and mechanical properties of boronized titanium alloy were investigated in [16]. Titanium alloy was boronized in both solid and liquid environments. Thanks to the boronizing process, the hardness value of Titanium alloy increased from 330 HV to 2800 HV. The abrasion resistance of Boronized Titanium alloy increased 17 times and 36 times in artificial body fluid. After the corrosion loss experiments, it was observed that the corrosion resistance increased from 1.2 times to 5 times with the increase in boronizing time. It was observed that boronized samples showed higher resistance to corrosive environments. It was revealed that boronized samples did not show toxic effects. It was understood that boronized Titanium alloy did not cause skin irritation.

Previous studies have been limited to quantitative measures such as abrasion volume loss, friction coefficient and corrosion rate of Titanium implant. In this study, the research has been taken further by measuring abrasion coefficients and polarization resistance, which are critical metrics in the evaluation of materials subjected to Tribocorrosion. The experimental results of Titanium implant materials have been extensively investigated and the issue of Titanium alloy as a possible replacement for commercially available implant materials has been investigated. In addition, SEM images of abraided Titanium materials have been taken and digital image processing techniques have been used to obtain better images and to extract morphological information of abraided parts. In addition, abrasion analysis of Titanium has been performed using digital image processing techniques and the role of alternative/supportive methods to laboratory environment analyses has been investigated. The remaining sections of the paper are structured as follows: In the second section, the methods applied in this study are discussed, the experimental procedures and techniques used are explained in detail. In the third section, the findings obtained during the research process are systematically presented and examined. In the last section, inferences are made in the light of these findings, the results obtained are interpreted in depth and the points reached throughout the study are evaluated.

2 Methodology

During the research, abrasion test, corrosion test, SEM images, Vickers hardness and abrasion depth measurement analysis of Ti6Al4V alloy supplied from two different companies were performed. Ti6Al4V samples were sized appropriately for abrasion, corrosion and Vickers hardness measurements. Secotom precision cutting device was used to size the samples. The precision cutting device is simple and flexible to use. It is

preferred for high quality parts and high capacity cutting processes. Precise cutting process can be applied for materials such as metals, composites, electronic parts, biomaterials, etc. Precise cutting process can be applied to materials such as metals, composites, electronic parts, biomaterials, etc. When applying the cutting process from the sample, precautions should be taken against the sample not to heat up too much and to prevent too much deformation. Coolant is used to minimize the heating that occurs when applying the cutting process to the sample. The liquid applied during the cutting process should not cause corrosion on the sample. The coolant used should remove the heat formed on the sample and the parts broken off from the sample from the cutting area. The cutting stages of the samples are shown in Fig. 1.

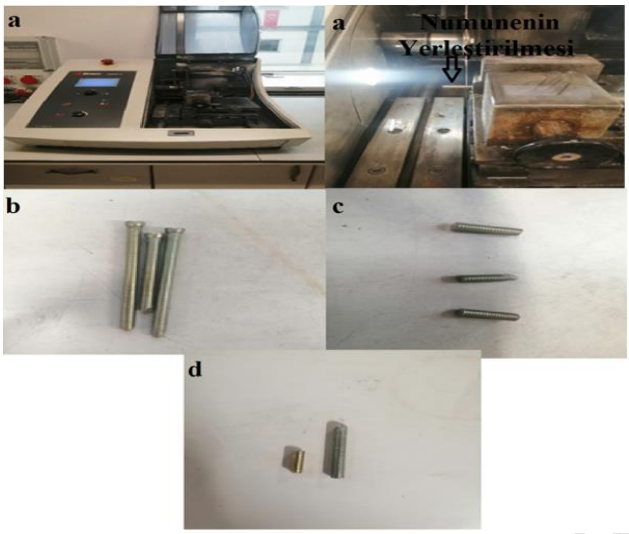

Figure 1. (a) Precision cutting device. (b) Ti6AI4V samples before cutting. (c) Samples prepared for abrasion test. (d) Samples prepared for corrosion test.

Samples cut to appropriate sizes are placed in the hot molding device using phenolic resin. The sample to be examined is placed in the chamber of the bakelite device in an appropriate manner. First, hot bakelite powder is poured onto the sample. The point to be noted here is that the powders should be compacted because when compaction occurs, the bakelite powder should pass the sample surface and it is also important that the bakelite powder completely covers the other surfaces of the sample. After the sample is placed, the sample and bakelite powders are kept at 150°C temperature and 30Mpa pressure for a certain period of time, then cooled and the sample is removed from the chamber. Resins such as bakelite, acrylic and epoxy are preferred when hot molding is applied. Phenolic resins are a thermoset plastic. After the cut samples are placed in the hot molding device and a certain amount of phenolic resin is added, the device is turned on and the sample is made ready. Fig. 2 shows the placement of the phenolic resin and samples in the hot molding device.

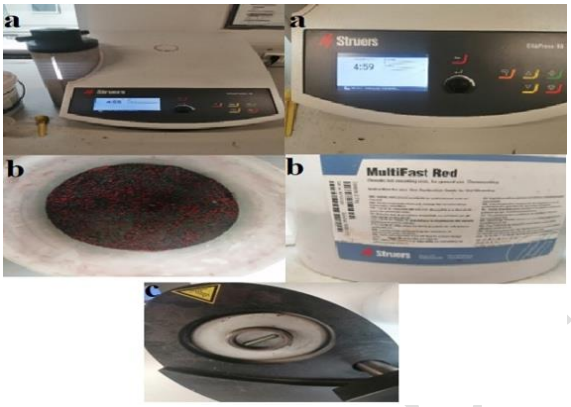

Figure 2. (a) Hot molding device. (b) Phenolic resin. (c) Placing the cut sample into the hot molding chamber.

The surfaces of the samples cut with precision cutting are scratched and rough. The sample should be sanded to remove this rough and scratched surface. The sanding process is done in order. In each order, the finer sanding is used than the previous one. In this way, the deformation and scratches formed on the samples are reduced to a minimum level. Sandpapers are obtained by sticking SiC, Al_2O_3 similar abrasives that are resistant to water, hard or fabric. Sandpapers are numbered according to the size of the abrasives. The numbering of sandpapers is done according to the number of abrasive grains. As the sandpaper number increases, the abrasive particle sizes on the sample surface decrease and the sandpaper becomes thinner. The sample is frequently cleaned with water to prevent the heating of the sample piece and to remove the broken pieces from the sample surface. When switching to a fine sandpaper, the sample should be turned 90°. When the sample is turned 90°, it is seen that the previous sanding traces disappear. When sanding, the sanding process is done for a longer time than the previous sanding paper was used. Each of the samples coming out of the hot molding device should be sanded one by one. P60D, P120D, P320C, P400C, P600C, P1000C, P1200 and 2500 papers were used for the sanding process, respectively. Fig. 3 shows the samples coming out of hot molding, before and after sanding and with sanding papers.

An artificial body fluid is a solution with an ion concentration close to that of human blood plasma, kept under mild conditions of pH and identical physiological temperature. An artificial body fluid contains mineral ions at concentrations nearly equal to those of human blood plasma Anodized Ti6A17Nb samples were exposed to simulated body. fluid, the preparation of which was optimized by Kokubo and Takadama. The body fluid was prepared by mixing 8 g NaCl, 0.3 g NaHCO3, 0.25 g KCl, 0.2 g K2HPO4.3H2O, 0.3 g MgCl26.H2O, 0.3 g CaCl and 0.072 g Na2SO4 compounds into ultrapure water, respectively, and then adding 45 mM tristampon solution and appropriate amount of HCl to stabilize the pH at 7.5 at 37 °C.

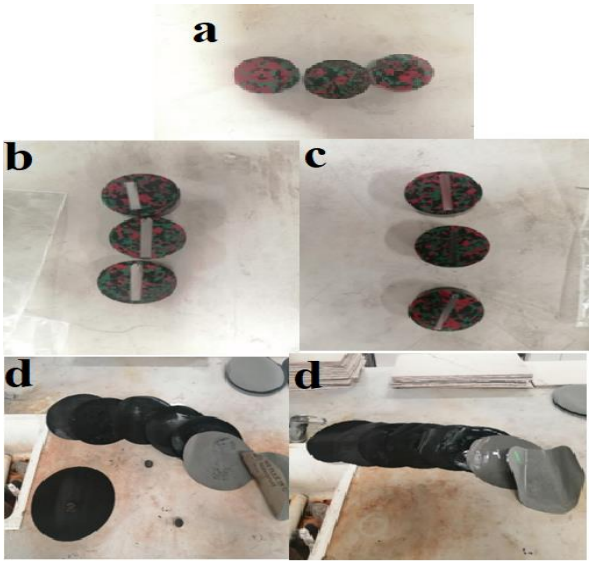

Figure 3. Prepared samples. (a) Samples coming out of hot molding. (b) Before sanding. (c) After sanding. (d) Sanding papers.

2.1 Abrasion Test

UTS Tribometer T10 test device was used in the abrasion tests. Tests in accordance with ASTM G-99 standard can be performed with this test device. Abrasion and friction behaviors can be examined by performing tests in accordance with ASTM G13 standard. Thanks to the corrosion cell, it allows the examination of abrasion and friction on materials in different corrosive environments (body fluids, basic solutions, etc.). Electro-Tribocorrosion test can be performed by adding a potentiostat. It provides high resistance of the material against corrosion and enables long-term use. It allows abrasion and friction tests to be performed on biomedical materials. The test device used for abrasion test is shown in Fig. 4.

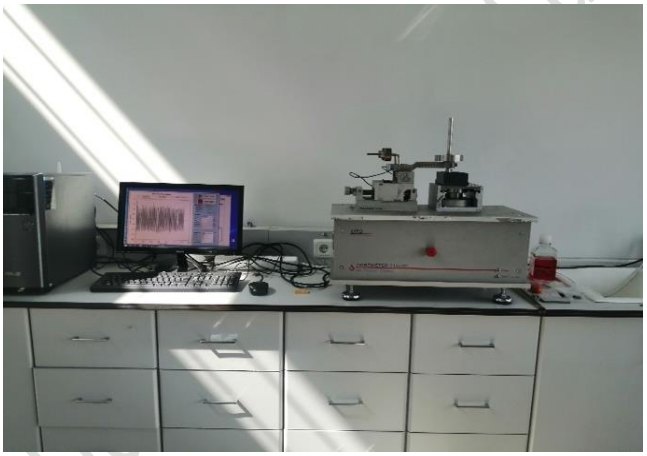

Figure 4. UTS Tribometer T10 tester.

In the abrasion tests, Ti6Al4V alloy samples obtained from three Ankara companies and three Gaziantep companies were used. For each test, errors that could be caused by surface deterioration were eliminated and the tests were carried out under the same conditions. The samples obtained from both companies were subjected to 10 N, 20 N and 30 N loads, respectively. The test phase of all samples was carried out at room temperature and using artificial body fluid. The speed of the abrasion test device was kept constant. Fig. 5 shows the preparation of the samples obtained from the companies and their placement in the test device.

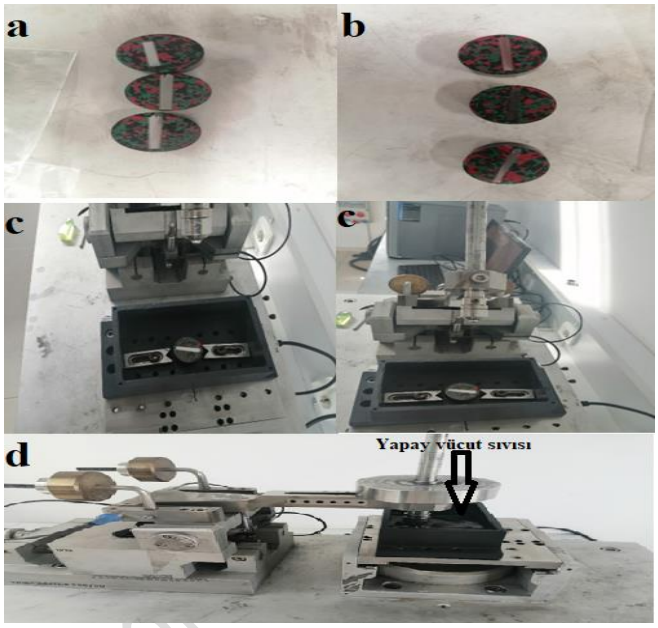

Figure 5. (a) Ankara sample. (b) Gaziantep Sample. (c) Placing the Samples. (d) Testing the Samples with artificial body fluid in the chamber for the abrasion test.

In Fig. 6, 10 N, 20 N and 30 N loads were applied to samples a, b and c, respectively.

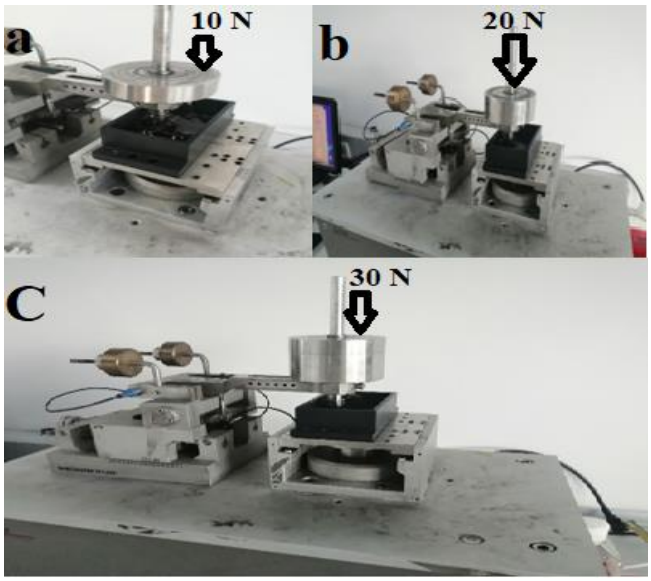

Figure 6. (a) Sample with 10 N load applied. (b) Sample with 20 N load applied (c) Sample with 30 N load applied.

All samples were cleaned with alcohol before and after the abrasion test. Fig. 7 shows the samples coming out of the abrasion tester after applying 10 N, 20 N and 30 N loads to the samples from two companies, respectively.

Figure 7. (a) Images of samples coming out of the abrasion tester after applying 10 N, 20 N and 30 N loads to Ankara samples, respectively. (b) Images of samples coming out of the abrasion tester after applying 10 N, 20 N and 30 N loads to Gaziantep samples, respectively

The average values of abrasion depth, friction coefficient and friction force of the samples after the abrasion test are shown in Fig. 8, Fig. 9 and Fig. 10, respectively.

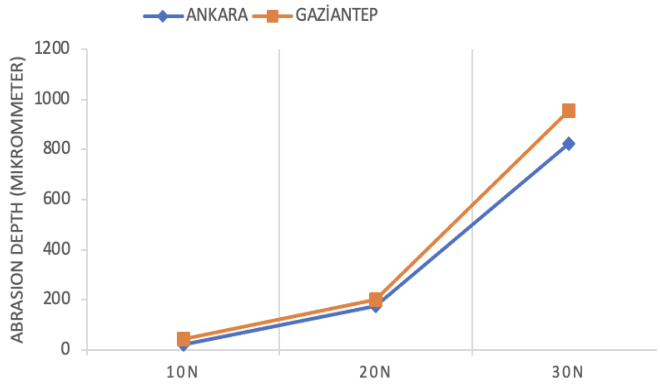

Figure 8. Average values of abrasion depth.

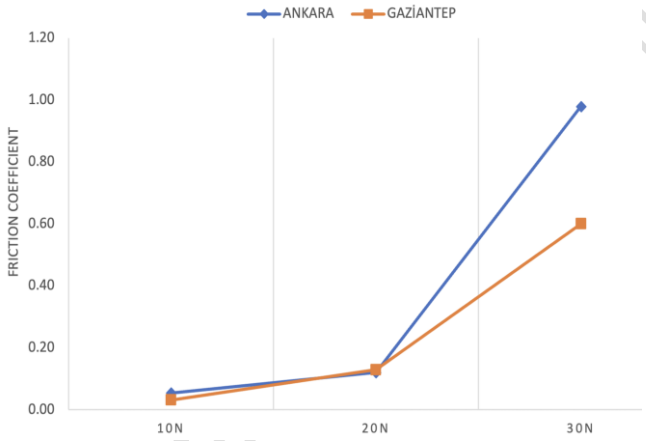

Figure 9. Average values of friction coefficient.

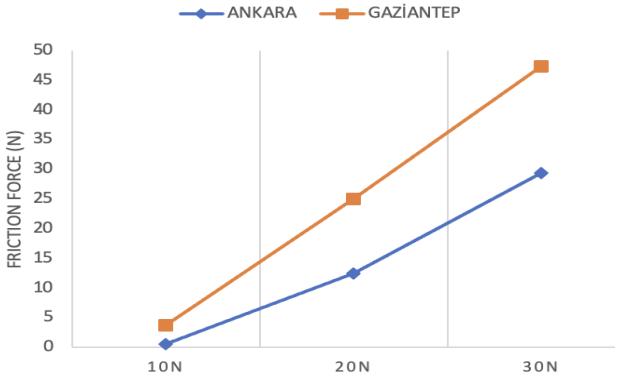

Figure 10. Average values of friction force.

2.2 Hardness Test

When force is applied to the surfaces of the sample to be measured, the sample must be fixed. The sample must be placed on the anvil surface in the hardness test and the sample surface must be raised to the tip of the indenter to be applied. The load is applied to the sample by increasing it and then removed. The samples obtained from both companies were prepared in hot molding devices in appropriate sizes and the Vickers hardness test was applied. The samples prepared for the hardness test and the devices used for the Vickers hardness test are shown in Fig. 11.

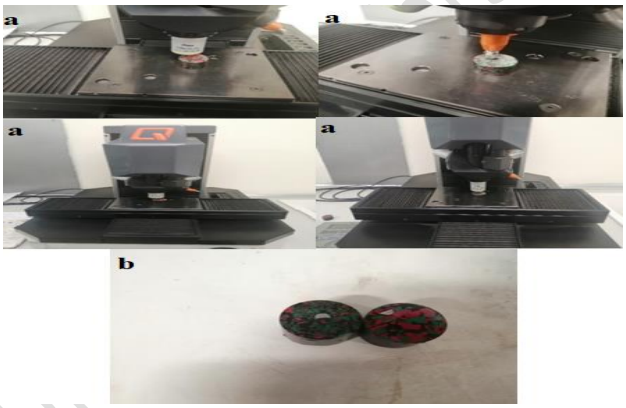

Figure 11. (a) Device used for Vickers hardness test. (b) Sample prepared for hardness test.

.The Vickers hardness test results of the samples obtained from Gaziantep and Ankara companies are shown in Table 1.

Table 1. Vickers hardness test results.

	GAZIANTEP	ANKARA
1.	340 HV	351 HV
2.	351 HV	352 HV
3.	322 HV	334 HV
4.	345 HV	322 HV
5.	336 HV	330 HV
6.	344 HV	335 HV
7.	366 HV	337 HV
8.	347 HV	341 HV
Average	343.875 HV	337.75 HV

As a result of the data obtained, the samples obtained from both companies are close to the average Vickers hardness of 340.51 HV for the Titanium alloy for the use of Ti6Al4V alloy.

2.3 Abrasion Scar Depth Test

The placement of the samples supplied by both companies in the device used to determine the abrasion scar depth is shown in Fig. 12.

Figure 12. Placing the samples in the device for abrasion scar depth.

The abrasion scar depths of the samples obtained from the wear test were measured in the order of Ankara 10 N, Ankara 20 N, Ankara 30 N, Gaziantep 10 N, Gaziantep 20 N, Gaziantep 30 N. The results of the measurements are shown in Table 2 and Table 3.

Table 2. Abrasion scar depth measurement results. (Ankara)

	10 N	**20 N**	**30 N**
1	245 µm	350.3 µm	378.6 µm
2	246.6 µm	370.5 µm	375.6 µm
3	305.3 µm	322.2 µm	396.1 µm
4	332 µm	375.9 µm	381.1 µm
5	324 µm	333 µm	378.8 µm
Average	290.58 µm	350.38 µm	382.04 µm

Table 3. Abrasion scar depth measurement results (Gaziantep)

	10 N	**20 N**	**30 N**
1	127.9 µm	300 µm	394 µm
2	159.2 µm	244.1 µm	333.6 µm
3	134.1 µm	280.3 µm	318.9 µm
4	164.7 µm	232.9 µm	414.2 µm
5	119.8 µm	281.3 µm	365.1 µm
Average	141.14 µm	267.72 µm	365.16 µm

2.4 Corrosion Test

The corrosion value of a certain surface is measured on the prepared samples. Before the cold bakelite process, the samples are cut to appropriate sizes for the preparation of the samples as in the abrasion test. They are placed in the hot molding device and the sanding process is applied. The cold bakelite is prepared in a cylindrical shape. The preparation of the samples, one of which belongs to Ankara and the other to Gaziantep, for the corrosion test is shown in Fig. 13.

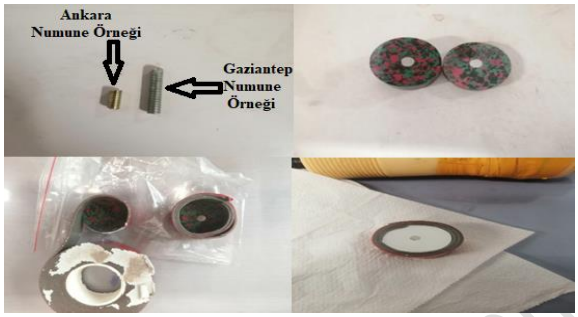

Figure 13. Samples prepared before corrosion test.

After the bakelite process is applied to the sample, the sample has upper and lower surfaces. In the lower part of the sample, a hole suitable for the flat-bottomed screw entrance is opened in the upper part of the sample to keep the sample stable during the test. The holder electrode is screwed to the flat-bottomed part of the sample and left in the test cell. One reference electrode and two graphite electrodes are placed in the cell. Then, artificial body fluid is added to cover half of the sample. The point to be noted is that the upper part of the sample should not come into contact with the solution. Before starting the test on the lower surface that will be exposed to corrosion, the area of the sample should be measured and the sample should be prepared according to the surface procedure. Before all tests, the open circuit potential of the sample in the corrosive environment is checked and then the necessary tests are performed. The corrosion test is shown in Fig. 14.

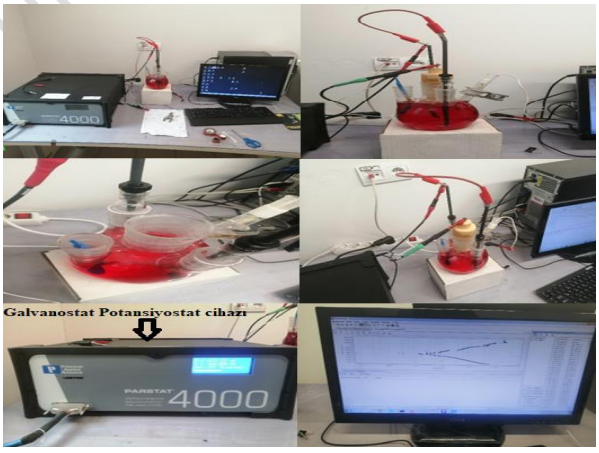

Figure 14. Laboratory used for corrosion test.

The parameters used for the corrosion test are shown in Table 4.

Table 4. The corrosion test parameters.

Samples	**Surface Area (cm^2)**	**Equivalent Weight (g)**	**Density (g/cm^3)**
Ankara	0.12	23.93	4.51
Gaziantep	0.12	23.93	4.51

2.5 Scanning Electron Microscope (SEM) Test

Scanning Electron Microscope (SEM) images of the titanium alloy after abrasion and corrosion were taken to investigate the potential of using image processing techniques in tribocorrosion applications. SEM images of the samples supplied by two companies were taken. Fig. 15 shows SEM images of the samples obtained from Ankara company after the abrasion test.

Figure 15. Ankara 10 N-1.00kx, 2.50kx, 5.00kx, 250x, 500x SEM images of the samples after the abrasion test, respectively.

Fig. 16 shows the SEM images of the samples obtained from the Gaziantep company after the corrosion test.

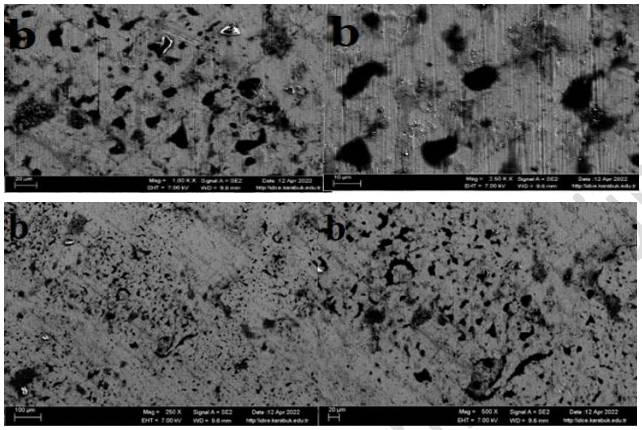

Figure 16. 1.00kx, 2.50kx, 250x, 500x images of the Gaziantep sample after the corrosion test, respectively.

3 Results and Discussion

3.1 Abrasion Test Results

The fixed parameters used for the abrasion test are frequency 3 Hz, stoke 10 mm, sliding distance 200 m, sliding speed 48.00 mm/s. The data in Table 2 and Table 3 were used for the abraided volume. Equation (1) was used to find the abrasion rate at the end of the abrasion test.

$$Abrasion\ Rate = \frac{Abraided\ Volume}{Applied\ Load * Sliding\ Distance} \quad (1)$$

Abrasion rate results are shown in Table 5.

Table 5. Abrasion rate results.

Company	Abrasion Rate
Ankara- 10 N	1.4529x10^{-3} mm^3/N*m
Ankara- 20 N	0.87595x10^{-3} mm^3/N*m
Ankara- 30 N	0.6337x10^{-3} mm^3/N*m
Gaziantep- 10 N	0.7057x10^{-3} mm^3/N*m
Gaziantep- 20 N	0.6693x10^{-3} mm^3/N*m
Gaziantep- 30 N	0.6086x10^{-3} mm^3/N*m

When the results obtained were evaluated, it was determined that the abrasion rate decreased as the applied force increased in the samples obtained from both companies. When the samples of both companies were compared with the applied forces respectively, it was determined that the wear rate of the screws of Ankara company decreased by 51% when 10 N load was applied, by 23% when 20 N load was applied, and by 4% when 30 N load was applied. The abrasion coefficient (c) was calculated using the formula in Equation (2).

$$c = \frac{Abrasion\ Rate * Vickers\ Hardness}{Applied\ Load * Sliding\ Distance} \quad (2)$$

The measurements in Table 1 were used for the abrasion coefficient calculation. The abrasion coefficient results calculated at the end of the abrasion test are shown in Table 6.

Table 6. Abrasion coefficient results.

Company	Abrasion Coefficient (c)
Ankara- 10 N	0.245358x10^{-3}
Ankara- 20 N	0.073963x10^{-3}
Ankara- 30 N	0.035840x10^{-3}
Gaziantep- 10 N	0.121336x10^{-3}
Gaziantep- 20 N	0.057538x10^{-3}
Gaziantep- 30 N	0.034880x10^{-3}

When the samples of both companies were compared with the applied forces, it was determined that the abrasion coefficient decreased by 51% when 10 N load was applied to the Ankara company, by 22% when 20 N load was applied, and by 2% when 30 N load was applied.

3.2 Corrosion Test Results

In the corrosion test, the corrosion rate can be calculated as in Equation (3).

$$Corrosion\ Rate = 3.27 * 10^{-3} * I_{corr} * \frac{E_w}{\rho} \quad (3)$$

In Equation 3, I_{corr} represents the corrosion current, E_w is the equivalent weight, and ρ is the density [17]. The corrosion rate results of the samples obtained from both companies are shown in Table 7.

Table 7. The corrosion rate results.

Samples	I_{corr} (μA)	Corrosion Current Density (i_{corr}) (μA/cm²)	Corrosion Rate (mm/year)	Corrosion potential (E_{corr}) (V)
Ankara	10.34	86.17	0.0047	-0.27
Gaziantep	57.91	482.58	0.005	-0.23

It was determined that the corrosion rate of the sample obtained from Ankara company was lower than the corrosion rate of the sample obtained from Gaziantep company.

3.3 Scanning Electron Microscope (SEM) Test Results

In Fig. 17 and Fig. 18, the segmentation process, one of the digital image processing techniques, was applied [18]. Digital image processing techniques were applied to the SEM images taken after the abrasion and corrosion tests of the samples. The MATLAB program was used during the segmentation process.

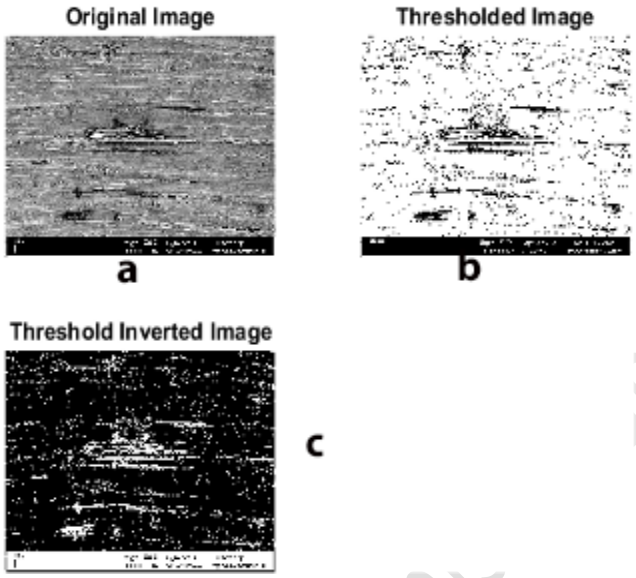

Figure 17. Applying segmentation process to Ankara 10 N abrasion sample image.

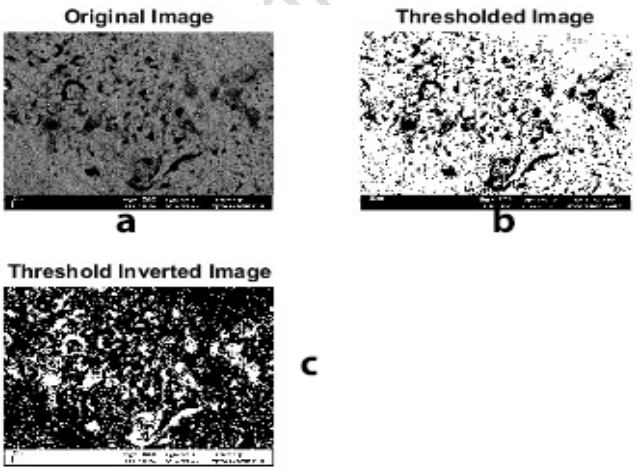

Figure 18. Applying segmentation process to Gaziantep corrosion sample image.

The segmentation process divided the image into clusters consisting of meaningful and similar sections. After segmentation, the image was defined as a cluster of interconnected and non-overlapping sections [19]. In this case, each pixel in the image had a single section label indicating the section it belonged to. Thanks to the segmentation process, the image was divided into objects and regions of the same type.

Histogram equalization is a popular image enhancement method to improve visual appearance of the image by assigning equal number of pixels to all available intensity values [20]. Histogram is a graph showing the number of pixel intensity values in an image. Histogram equalization is a method used to eliminate pixel intensity distribution disorder caused by the clustering of pixel intensity values in a certain place in an image. Histogram equalization was applied to the SEM images taken after the abrasion and corrosion tests of the samples in Fig. 19 and Fig. 20. The MATLAB program was used for histogram equalization.

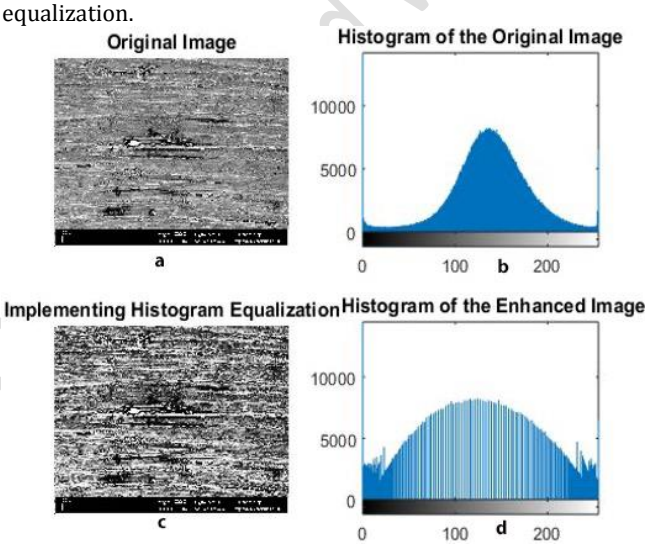

Figure 19. Applying histogram equalization to Ankara 10 N abrasion sample image.

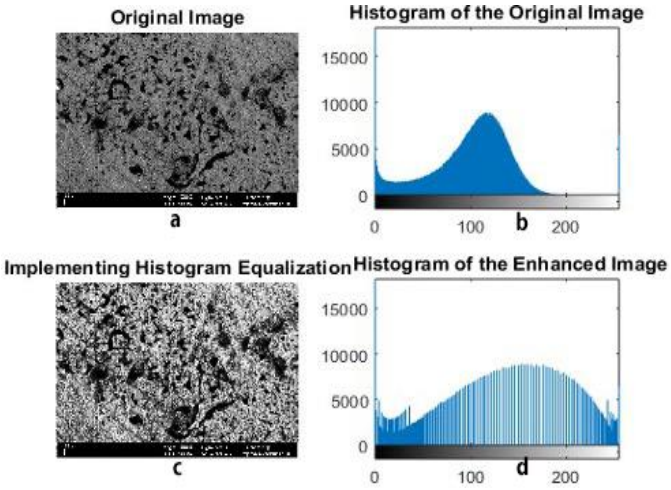

Figure 20. Applying histogram equalization to Gaziantep corrosion sample image.

Histogram equalization applied images contain important information [21]. The histogram of a dark image will be concentrated in the lower gray level region. The histogram of a bright, smooth image will be concentrated in the higher gray level zone. If the histogram is spread over a region, the contrast

of this image is bad. The histogram graph of an image with good contrast shows that it is spread equally over all gray level values. Low visibility on the image is improved with histogram equalization.

Edge detection on an image can be used to detect, count and determine the properties of objects in that image. Edge detection algorithms are most basically determined by the differences in the color values of pixels on the image. These differences are called transitions and represent the edge lines for us. In this section, each algorithm can detect by making its own inferences. In Fig. 21 and 22, you can see an image with the edge extraction algorithm applied.

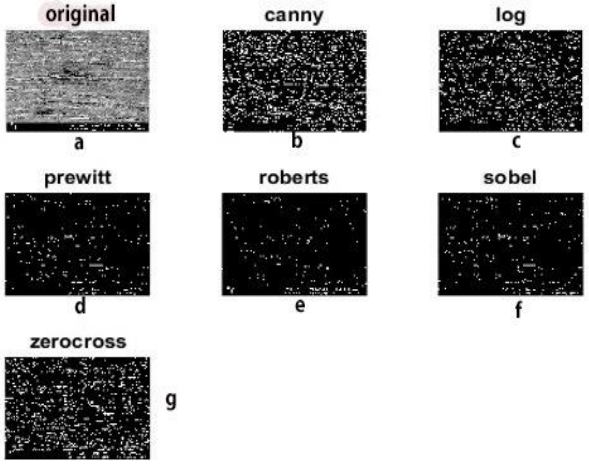

Figure 21. Applying edge detection process to Ankara 10 N abrasion sample image

The Canny algorithm uses four filters to detect horizontal, vertical and diagonal edges in the blurred image. The image is filtered by the kernel to obtain the first derivative in both horizontal and vertical directions. Roberts, Sobel and Prewitt are Gradient-based edge detection and involve finding the gradient of the image intensity function. The gradient measures the rate of change of intensity, and edges are typically located where this rate of change is maximized. Laplacian of Gaussian (LoG) and Zero-cross are Gaussian-based edge detection and involve smoothing the image with a Gaussian filter to reduce noise and then detecting edges, often using second-order derivatives. In Fig. 21 and Fig. 22, the edge detection process from digital image processing techniques was applied to the samples with the help of the MATLAB program. Using the edge detection method, discontinuities in the depth of the images, orientations on the sample surface and changes in material properties were examined. Thanks to the edge detection algorithm, a path is created corresponding to the boundaries of the objects, the boundaries of the surface marks and discontinuities in the surface orientation.

When the results obtained in this paper are compared with the literature studies, both [11] and this paper aim to enhance the performance of the Ti6Al4V alloy in biomedical applications through surface modification. SEM analyses were used for the detailed examination of surface properties. In [11], surface modification (sandblasting and laser) was performed to enhance biocompatibility, whereas this paper focuses on tribocorrosion analysis. This study examined surface properties after abrasion and corrosion using digital image processing techniques, whereas this method was not used in [11]. [11] examined biocompatibility and surface roughness; this paper provided a detailed analysis of tribocorrosion mechanisms. While [12] focused on examining the mechanical and microstructural properties of the Ti-6Al-4V alloy after its production using additive manufacturing methods, this paper evaluated the tribocorrosion resistance and surface properties of the Ti-6Al-4V alloy for biomedical implants. In [13], coating methods for Ti-6Al-4V surface modification were presented, and the effects of innovative materials such as graphene were evaluated. In contrast, this paper examined surface enhancement methods aimed at improving the tribocorrosion performance of Ti-6Al-4V in biomedical applications. In the study [16], the focus was on biocompatibility and mechanical properties after the boronizing process. It improved parameters such as biocompatibility and hardness, However, this study emphasized the simultaneous effects of abrasion, corrosion and imaging techniques. It analyzed implant durability by detailing surface properties.

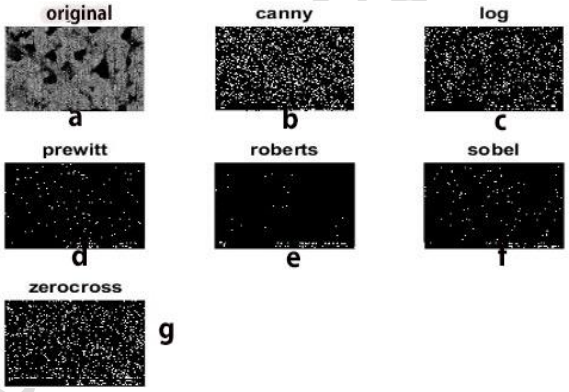

Figure 22. Applying edge detection process to Gaziantep corrosion sample image.

4 Conclusion

The tribocorrosion properties of titanium alloy were investigated by applying digital image processing techniques to SEM images obtained after abrasion and corrosion tests. Commercial Ti6Al4V alloys produced by two different companies were tested in simulated artificial body fluid and it was observed that the abrasion rates of samples obtained from Gaziantep company were more stable than Ankara company. As a result, it was concluded that Ankara company's products had longer life. Adhesion abrasion was detected in SEM images, and the depth and number of pits increased with the increase in applied loads. Abrasion and corrosion areas were clearly segmented with digital image processing techniques and color distribution was improved with histogram equalization. Abrasion and corrosion areas were highlighted with edge detection method and unimportant information was filtered. As abrasion increases in the titanium alloy, ion release in the body of the samples will increase, which may cause various diseases in the future. Surface coating methods can be developed to prevent abrasion and corrosion for titanium alloys. Since abrasion and corrosion limit the life of the titanium alloy, extending its life has become a critical importance. Newly designed alloys and new biomaterials such as biodegradable materials need to be developed for medical applications. It should be noted that the study has the limitation of long-term in vivo testing. That is why the study can be extended by experiments of long-term in vivo tests. Moreover, the results of this study can be extended by performing the same test under dynamic loading conditions and exploring additional surface treatment methods.

5 Acknowledgment

This study was supported by the Scientific Research Projects Coordination Unit of Alanya Alaaddin Keykubat University with the project number 2021-02-10-LTP01.

6 Author contribution statements

In the scope of this study, the Author 1 in the formation of the idea, the design and the literature review, the assessment of obtained results, supplying the materials used and examining the results; Author 2 in the writing and critical review, spelling and checking the article.

7 Ethics committee approval and conflict of interest statement

There is no need to obtain permission from the ethics committee for the article prepared.

There is no conflict of interest with any person / institution in the article prepared.

8 References

[1] Ünal E, Karaca F. "Ti-6AI-4V alaşımının dik işlem merkezli CNC tezgahında işlenebilirliğinin araştırılması". *Fırat Üniversitesi Doğu Araştırmaları Dergisi*, 6(1), 135-139, 2007.

[2] Taş A. C. "Synthesis of biomimetic Ca-hydroxyapatite powders at 37^{0}C in synthetic body fluids". *Biomaterials*, 21(14), 1429-1438, 2000.

[3] Kazancıoğlu H, Kılıç S, Ak G. "Titanyum dental implantlarda korozyon", *Atatürk Üniversitesi Diş Hekimliği Fakültesi Dergisi*, 24(8), 82-87, 2015.

[4] Luo Y, Jiang H, Cheng G, Liu H. "Effect of carburization on the mechanical properties of biomedical grade titanium alloys". *Journal of Bionic Engineering,* 8, 86-89, 2011.

[5] Irmak E, Uğurlu B, İncesu A. "Investigation of tribocorrosion properties of titanium implant used in orthopedics". *2022 Medical Technologies Congress (TIPTEKNO),* Antalya, Turkey, 31 October-02 November 2022.

[6] Rosenfeld A. *Picture processing by computer*, New York, Academic Press, 1969.

[7] Şap B, Şap E, Kırık İ. "Titanyum ve alaşımlarının biyomalzeme olarak kullanılması". *III. Uluslararası Battalgazi Bilimsel Çalışmalar Kongresi*, Malatya, Türkiye, 21-23 Eylül 2019.

[8] Urtekin L, Keleş Ö. "Biyomedikal Uygulamalar İçin TiN Kaplı Ti6Al4V Alaşımının Mekanik Özelliklerinin Araştırılması", *Savunma Bilimleri Dergisi*, 18(36), 91–108, 2019.

[9] Gökdemir Y. Saf Titanyum ve Ti6AL4V Alaşımının Yüksek Sıcaklıkta Oksidasyon Davranışı. Yüksek Lisans Tezi, İstanbul Teknik Üniversitesi, İstanbul, Türkiye, 2005.

[10] Vurat M. T. Titanyum İmplant Uygulamalarına Yönelik Osteojenik Yüzey Nanokaplamalarının Geliştirilmesi, Yüksek Lisans Tezi, Ankara Üniversitesi, Ankara, Türkiye, 2016.

[11] Yıldız H. Biyomedikal uygulamalarda kullanılan Ti6Al4V alaşımının yüzey modifikasyonu ve in vitro biyoaktivitesinin incelenmesi, Yüksek Lisans Tezi, Yıldız Teknik Üniversitesi, İstanbul, Türkiye, 2010.

[12] Memu F. Katmanlı İmalat Yöntemiyle Ti-6AI-4V Alaşımının Mekanik Özelliklerinin İncelenmesi, Yüksek Lisans Tezi, TOBB Ekonomi ve Teknoloji Üniversitesi, Ankara, Türkiye, 2019.

[13] Özkan O. Saf Titanyum (CP-Ti) ve Titanyum Alaşımının (Ti-6AI-4V) Yüzey Özelliklerinin Geliştirilmesi, Yüksek Lisans Tezi, Bilecik Şeyh Edebali Üniversitesi, Bilecik, Türkiye, 2019.

[14] Arslan Ş. Ti6al4v Titanyum Alaşımının Lazer Kaynak Kabiliyeti ve Biyoaktivite Özelliklerinin İncelenmesi, Yüksek Lisans Tezi, Karabük Üniversitesi, Karabük, Türkiye, 2020.

[15] Ateş G. Ti6Al4V Titanyum Alaşımının İç Yapısı ve Yüzey Özellikleri Üzerine Termokimyasal İşlem Parametrelerinin Etkisi, Yüksek Lisans Tezi, Süleyman Demirel Üniversitesi, Isparta, Türkiye, 2018.

[16] Kaplan Y. İmplant Yapımında Kullanılan Ti6Al4V Titanyum Alaşımının Mekanik Özelliklerine ve Biyouyumluluğuna Borlama İşleminin Etkisi, Doktora Tezi, Pamukkale Üniversitesi, Denizli, Türkiye, 2017.

[17] Turan M.E, Aydin F. "Wear and corrosion properties of low-cost eggshell-reinforced green AZ91 matrix composites". *Canadian Metallurgical Quarterly,* 61(2), 155-171, 2022.

[18] Uçurum M, Güneşsu E, Şirin T. B, Kaynak Y. "Farklı kesme parametreleriyle işlenmiş 316LVM paslanmaz çelik malzemesinin talaşlı imalat-yüzey bütünlüğü-aşınma direnci arasındaki ilişkinin incelenmesi". *Pamukkale Üniversitesi Mühendislik Bilimleri Dergisi,* 27(4), 449-457, 2021.

[19] Ünlü B. S, Köksal S, Atik E, Meriç C. "CuSn10 yatak malzemesinin tribolojik özelliklerinin incelenmesi". *Pamukkale Üniversitesi Mühendislik Bilimleri Dergisi,* 11(1), 41-45, 2005.

[20] Irmak E, Erçelebi E, Ertaş A. H. "Brain tumor detection using monomodal intensity based medical image registration and MATLAB". *Turkish Journal of Electrical Engineering and Computer Sciences*, 24(4), 2730-2746, 2016.

[21] Candemir D, Karacif K, Kartal L. "Investigation of the corrosion properties of AA5754 aluminum alloy coated with graphene oxide by the electrophoretic deposition method". *Pamukkale Üniversitesi Mühendislik Bilimleri Dergisi,* 30(1), 10-16, 2024